On resource efficient and individualized tree support structures for PBF-LB/M by process simulation

Jan Hünting[1*] 0009-0000-7484-4992, Jochen Michael[2] 0009-0006-4878-3632, Claus Emmelmann[1] 0009-0008-4698-2077, Tim Röver[1] 0000-0002-3709-339X

[1] Hamburg University of Technology, Hamburg, Germany
[2] CENIT AG, Stuttgart, Germany

* Corresponding Author: jan.huenting@tuhh.de, +49 40 42 878 - 4422

Abstract

Laser powder bed fusion of metals (PBF-LB/M) is a widely used additive manufacturing process known for its ability to create complex geometries with high precision. However, the necessity of support structures in PBF-LB/M leads to significant material and energy consumption, impacting overall efficiency. This work investigates a novel approach combining numerical process simulation with a user-friendly software tool to design resource-efficient tree support structures. A demonstrator part, manufactured from Ti6Al4V titanium ally, is used to validate the effectiveness of these generative support designs. The accuracy of the process simulation is assessed by comparing numerical results with geometrical deviations, obtained by 3D scanning the additively manufactured demonstrator parts. Additionally, the newly designed support structures are compared against widespread block supports, focusing on material consumption and geometrical precision. The demonstrator with tree supports shows 34.48 % less mean deviation than the one with block supports while being slightly lighter. These results demonstrate that the presented approach allows for the creation of individualized and efficient tree support structures, leading to faster print preparations, less misprints and therefore reduced manufacturing costs. Moreover, new manufacturing limits for thin rods in PBF-LB/M are identified by the successful fabrication of 50 mm long rods with minimum diameters of 0.3 mm and inclination angles to the built plate greater than 20 °, as well as vertical rods up to 300 mm in length. This increases the design freedom for components and support structures in PBF-LB/M processes drastically. Overall, the integration of advanced support design techniques shows promise for enhancing the sustainability and cost-effectiveness of PBF-LB/M.

Keywords: additive manufacturing (AM); laser powder bed fusion of metals (PBF-LB/M); tree support structure; design guideline; titanium alloy Ti6Al4V; generative design

1 Introduction

Laser Powder Bed Fusion of Metals (PBF-LB/M) is a widely adopted additive manufacturing (AM) technology, particularly valued for its ability to produce highly complex geometries with high precision and excellent mechanical properties [1], [2]. This process has found critical applications in industries such as aerospace, healthcare, energy, and automotive, where customized, lightweight, and mechanically robust components are in high demand [3], [4], [5]. While PBF-LB/M offers substantial advantages over traditional manufacturing, the process faces challenges that limit its efficiency and sustainability, such as potentially high residual stresses and anisotropic mechanical properties [6], [7].

One of the most significant challenges in PBF-LB/M is the necessity of support structures, which stabilize overhanging features during manufacturing, dissipate heat and mitigate thermal stresses to prevent part deformation [8]. These supports are essential for ensuring stable processes and geometrically accurate parts but contribute significantly to material and energy consumption, increased manufacturing times and extensive post-processing, thereby inflating overall production costs [9]. Traditional support types, such as block and lattice supports, often result in inefficient material usage and can be challenging to remove, highlighting the need for optimized solutions. Addressing these inefficiencies is a key priority for advancing the sustainability and cost-effectiveness of PBF-LB/M.

To overcome these limitations, recent research has focused on optimizing support structures through advanced design techniques, such as topology optimization and generative design algorithms [10], [11]. Among these innovations, tree-like support structures have gained attention for their potential to reduce material usage and simplify post-processing [12], [13]. Inspired by natural branching patterns, tree supports offer minimal contact points with the manufactured part, facilitating easier removal and reducing the risk of surface damage [14]. These supports have been shown to perform effectively in managing complex geometries and overhangs, making them highly suitable for a variety of

AM applications [15], [16], [17]. The development of tree-like supports is expected to significantly improve the sustainability and cost-effectiveness of AM processes [9], [18].

This study builds upon prior developments in tree-like supports by integrating numerical process simulations with a user-friendly software tool for the design of tree supports. By combining generative design with simulation-based optimization, this approach aims to create resource-efficient and individualized support structures tailored to specific geometries and manufacturing conditions. To validate the methodology, a demonstrator part was produced using Ti6Al4V titanium alloy, and the performance of tree-like supports was compared against commercially wide spread block supports. Key evaluation metrics are material consumption and geometric accuracy. Additionally, a parameter study on thin rods made out of titanium alloy Ti6Al4V is conducted to expand the manufacturing limits and increase the general design freedom of the PBF-LB/M process.

The integration of advanced simulation tools with innovative design methodologies represents a significant step toward enhancing the overall efficiency of PBF-LB/M. This work not only addresses critical limitations associated with traditional support structures but also provides a pathway for improving the sustainability and precision of AM processes. The findings presented in this study contribute to ongoing efforts to expand the design freedom, reduce resource consumption, and lower overall production costs in the field of additive manufacturing.

2 Related works

A software tool for the generation of tree supports was developed in previous works. It allows the creation of material and energy efficient support structures without much user experience. It could be shown that material savings of the support structures of up to 85 % are possible when simulatively compared to block supports, while exhibiting comparable displacements [15]. Additionally, the software tool enables the export of the generated tree supports as volume models in the *Standard for the Exchange of Product Data format* (STEP). In contrast to the prevailing tessellated formats, the STEP format allows the subsequent manipulation of the supports in arbitrary Computer aided Design (CAD) softwares as well as the effective integration into the toolpath planning of most common computer aided manufacturing planning tools for automated and efficient post-processing [12]. Waldschmidt et al. [13] used the software tool in their latest publication to generate resource-efficient and tree-like add-on structures with the goal of simplifying the automated, mechanical postprocessing of AM parts. The software tool leads to the fast generation of well adapted, material efficient and flexible tree support structures. See [15] and [19] for further details of the developed software tool and section 4.2 for advancements and changes in the code.

3 Methodology

The work at hand aims to deepen and expand the findings on the developed tree generation software tool. A parameter study on thin rods with varying diameters, lengths and angles of inclination was conducted to validate the standard parameters in the software tool and a small design guideline for thin rods manufactured in Ti6Al4V by PBF-LB/M is presented from the results. A demonstrator part from the aerospace sector was used to showcase an optimized process chain including process simulations and the adjustment of the generated tree supports. The demonstrator model was then printed once with the adjusted tree supports as well as once with commercially widespread block supports and both demonstrators were 3D scanned subsequently. Additionally, the weight of both support types was measured, which allows the comparison between them, based on the process simulations and the scanning results. Moreover, the results from the scans and the simulations were compared to evaluate the predictive accuracy of the simulation model used in this work.

3.1 Parameter study

The test component of the parameter study consists of 44 thin circular rods with varying diameters, lengths and inclination angles to the built plate. Table 1 shows the design of experiment including all parameter combinations considered in this study and a picture of the printed study can be seen in Figure 1.

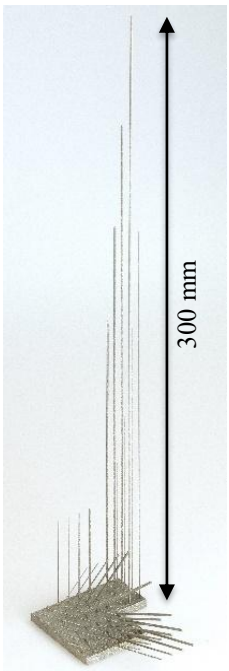

Figure 1: Parameter study on thin rods manufactured by AM. The scale is given by the tallest rod with a height of 300 mm.

To evaluate the study, the accuracy of the printed rods in terms of inclination angles and lengths was measured. Several 3D scanning systems were tested for this purpose but failed to catch the intricate geometries. Therefore, a protractor and a caliper gauge were used. The measurement errors of these devices were tested by repeating measurements, resulting in an angular error of 0.46 % and a dimensional error of 0.56 %, respectively.

3.2 Process chain

An optimized process chain for the AM of metallic parts has been developed by Hünting et al. in [12]. The adapted version of this process chain is shown in Figure 2. It starts with

the generation of tree support structures, which can then be optimized in an iterative loop (represented by the dashed line in Figure 2) using process simulation. When the iteration loop is finished, the part is additively manufactured, followed by a stress relieving heat treatment and the manual support structure removal.

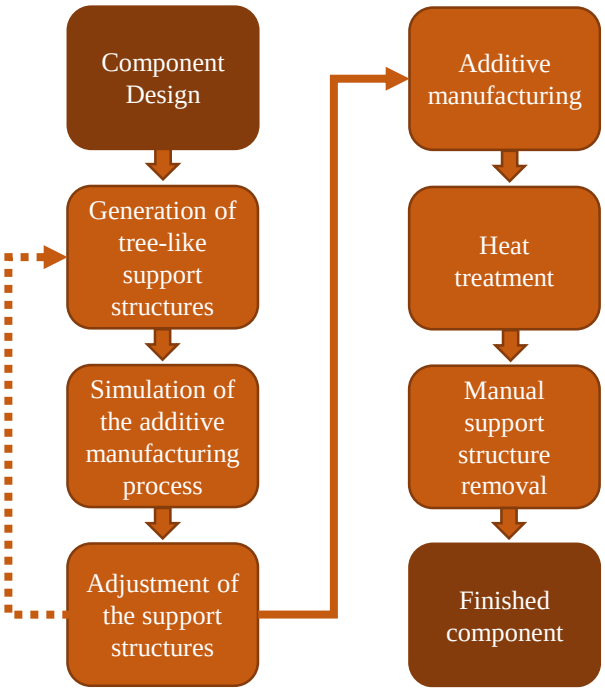

Figure 2: Flowchart of the optimized process chain for the additive manufacturing of metallic parts.

This process chain enables the creation of well-adapted and reliable support structures. Application of the optimized process chain to the demonstrator part is presented in the sections 4.3 and 4.4 of this work.

3.3 Process simulation

The process simulations of this work are finite element analyses that were performed in *Netfabb Local Simulation 2023* from *Autodesk* [20]. The material properties of Ti6Al4V are taken from the software´s *material library* and the *Nikon SLM500* machine with four lasers was selected. An adaptive mesh, consisting of cubic voxels of different sizes, was created using a padding tolerance of 0.05 mm. The minimal wall thickness value was set to 0.13 mm for the block supports and 0.24 mm for the tree supports. These rather fine mesh settings lead to elongated computation times but are necessary because of the delicate features of the block supports. All simulations are carried out with the *support structure failure criteria* set to 1050 MPa. The steps of each process simulation include the PBF-LB/M process, a standard stress-relief heat treatment for two hours at 700 °C and the removal from the built plate, followed by the removal of the support structures.

For further details on the chosen laser and process parameters of the process simulations the reader is kindly referred to [15].

3.4 Additive manufacturing

Both demonstrators (with block and tree support) and the parameter study were manufactured in a single printing process by the *Fraunhofer IAPT* on a *Nikon SLM500 quad* PBF-LB/M machine [21]. The machine features a build envelope of 500 x 280 x 365 mm^3, Ti6Al4V was used as material and the layer thickness was set to 60 µm. Refer to Figure 1 for the printed parameter study and to Figure 4 for the printed demonstrator models.

Subsequently to the printing itself, all parts were carefully extracted from the powder bed, the parts were removed from the built plate via wire erosion under water and remaining powder was removed from the components. Both demonstrator parts were subjected to a heat treatment before the support structures were removed manually.

3.5 Measurement of geometric deviations

Due to the organic and complex geometry of the demonstrator model, it was not feasible to measure the geometric accuracy with conventional measurement equipment. Alternatively, the 3D scanning system *VL-500 coordinate measuring machine* from *Keyence* was used for that purpose. It has a geometric accuracy of ± 10 µm and the associated scanning software *Keyence VL-500 Application Series* provides the possibility to combine scans from different angles, create 3D CAD comparisons and analyse the scanning data [22].

4 Results and discussion

In this section, the results of this work are presented and discussed.

For more detailed information on the software tool and the analysis done in this work, the reader is kindly referred to the supplementary material [23]. It contains the source code of the software tool, a complete list of all improvements on the tool, pictures from the 3D scanning process and of the demonstrators from other perspectives. Additionally, the locations of all reference points and a complete table of all local deviations (scanned and simulated) at these reference points are included.

4.1 Parameter study

35 out of the 44 rods of the parameter study were fabricated successfully within the tolerances of the measuring instruments (Figure 1).

The results of the analysis can be found in Table 1. Multiple values within a single cell indicate that the result applies to all possible combinations in the corresponding row. It shows that the PBF-LB/M process is able to manufacture Ti6Al4V rods with lengths of 50 mm

successfully as long as diameters are greater than 0.3 mm and angles of inclination between the rods´ mid axes and the built plate are greater than 20 °. Additionally, all the vertical rods with lengths between 70 mm and 300 mm were printed successfully.

In contrast, the rods with a diameter of 0.1 mm were either not printed at all or were broken at certain lengths. The rods with a diameter of 0.2 mm and inclination angles to the built plate of 20 °, 30 ° and 90 ° were broken, whereas the remaining rods (25 °, 45 °, 60 °) were successfully built. The angular deviations of the broken rods were not measured.

Table 1 Manufacturability of thin rods from Ti6Al4V with a length of 50 mm and various diameters and angles of inclination.

Design		**Measurement**	
Diameter [mm]	Inclination angle [°]	Length [mm]	Manufactured successfully
0.1	20	0	✗
	25	0	✗
	30	2	○
	45	13	○
	60	0	✗
	90	0	✗
0.2	20	18	○
	25	50	✓
	30	31	○
	45	50	✓
	60	50	✓
	90	2	○
0.3, 0.5, 0.7, 0.9	20, 25, 30, 45, 60, 90	50	✓
0.5	90	70, 100, 150, 200	✓
1.0	90	150, 200, 250, 300	✓
Legend:	✓	printed successfully	
	○	broken or bent	
	✗	not printed	

There are multiple possible reasons for the unsuccessful manufacturing of some of the rods. It is possible that thin rods could not be properly manufactured in the PBF-LB/M process. Furthermore, it could be that thin rods were successfully manufactured in PBF-LB/M but the filigree structures have been damaged during the extraction of the component from the powder bed, during the wire erosion from the built plate or during transportation.

These findings are in line with results from literature regarding PBF-LB/M with Ti6Al4V and even surpass them in some aspects. Aputharaj et al. conducted a similar parameter study in 2023 but restricted the lengths of the rods to 10 mm. They stated manufacturability of rods with a minimum diameter of 0.3 mm for even smaller inclination angles of 10 ° [24]. A paper from 2015 investigated rods with a length of up to 80 mm and found them to be manufacturable with minimum diameters of 0.5 mm and inclination angles of 30 ° [25]. To our knowledge, no previous study investigated manufacturability of Ti6Al4V rods that are longer than 80 mm in PBF-LB/M. In this study we report successful manufacturing of thin rods up to 300 mm in length.

4.2 Improvements to the tree support generation tool

Several improvements and enhancements were implemented to the tree support generating software tool since it was presented in [15], including bug fixes, optimisations of the graphical result output and a reduced calculation time by approximately 50 %. Additional parameters for an even more individualized *standard tessellation file* (STL) export were added, enabling the user to choose the accuracy of the meshing. When exporting the supports as STEP files, it is now possible to merge all branches into a single object as well as to export the tree support as a stand-alone object.

Furthermore, changes to the generation of the tree supports are implemented. Support branches and trunks that are longer than a selectable maximum branch length get their radii thickened by 25 %. Trunks that exceed the maximum branch length by a factor of 1.5 or more are executed with a conical shape. The results of the parameter study (section 4.1) were used to set the software tool´s standard parameters (e.g. maximum branch length of 50 mm). Additionally, a new parameter concerning the maximum diameter of the tree crown was added, enabling the user to choose the size and therefore the number of trees generated as well as to avoid first level branches that are too long or too horizontal. To achieve an easier support structure removal, the attachment geometry of the tree supports to the component was modified depending on the type of connection to the component. The branch ends are designed as hemispheres, when the branch connects to a component´s surface. They are designed as cones, when the branch connects to a component´s point or edge. To increase the flexibility and adaptability of the software tool even further, an import function was implemented that allows the import of highly stressed points which can be obtained from process simulations. Additional branches with cones at their ends are then connected to these points to ensure easy removability.

The behaviour of the software tool can be controlled by nearly 30 parameters in total, which are stored in a customizable configuration file.

4.3 Support structure generation and adjustment

The adapted process chain (Figure 2) was followed for the generation and adjustment of the tree support structures for the demonstrator part. The demonstrator model was imported into the software tool and tree supports were generated (left picture of Figure 3) using the standard parameter set, developed in [15]. The generated tree supports were saved as STL file and a process simulation was set up with this model as explained in section 0. Then the iteration loop of the process chain was entered by analysing the simulation results with regard to the geometrical distortions occurring during the whole process and especially after completion of all manufacturing steps. It was determined that some areas of the demonstrator part were not sufficiently supported, whereupon the supports were then adjusted according to the simulation results.

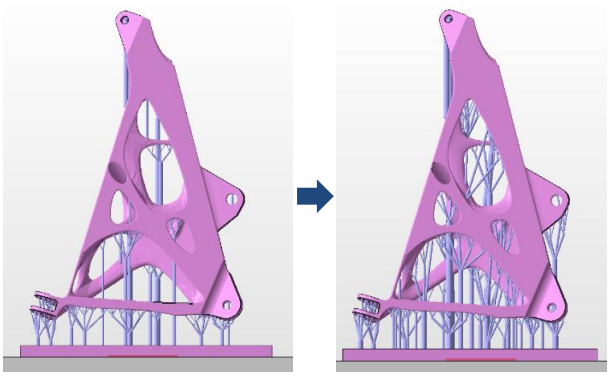

Figure 3: Generated (l.) and adjusted (r.) tree support structures on the demonstrator part

To do this, highly stressed points from the process simulation were exported first. To ensure a minimum space between support branches a threshold of minimum distance was applied, deleting some points from the data set. The remaining points were then imported into the software tool, increasing the number of generated trees. The newly implemented crown diameter was decreased from 25 mm to 15 mm to generate smaller tree crowns and therefore more trunks to compensate for the higher number of branches. To increase the general stability of the supports, the radius factor was increased from 0.8 to 0.9 and the starting radius was increased from 0.2 mm to 0.25 mm. Lastly, a few branches that were too close to each other, were deleted and one trunk was thickened manually to compensate for high distortions predicted by the simulation. These manual adjustments are solely possible because of the STEP export function of the software tool and improve the flexibility and adjustability of the generated tree supports drastically. The demonstrator with the adjusted tree supports is shown in the right picture of Figure 3.

The block supports were generated by an expert for additive manufacturing of the *Fraunhofer IAPT*, using the software *Magics* from *Materialise* and are shown in the left picture of Figure 4.

4.4 Additive manufacturing

The additive manufacturing was done according to section 3.4. The support structures of both demonstrator parts were removed manually using a pliers. In case of the tree supports, the degree of difficulty of the removal varied significantly depending on the feature. The first level branches were relatively easy to detach but a considerable amount of support residue remained on the surfaces. Some of these branches were located in hard-to-reach areas of the component, complicating the removal process. The most difficult feature to remove were the thick trunks. Ideally, these trunks should terminate on the build platform rather than the part, which was not consistently the case (right pictures of Figure 4).

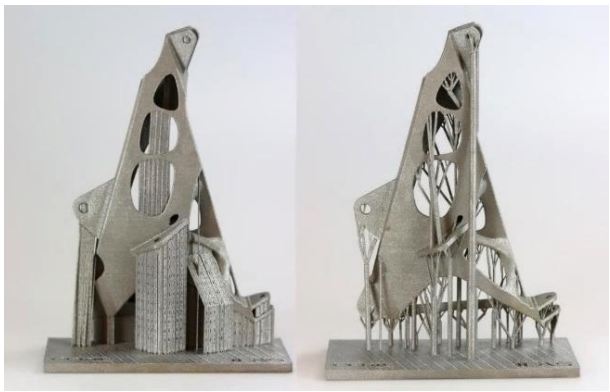

Figure 4: Additively manufactured demonstrator part with block supports (l.) and tree supports (r.)

In general, the contact geometry of the block supports allowed for slightly easier removal from both the part and the build platform, though a similar amount of support residue was left on the part. Areas in which the supports were densely packed posed greater difficulty during removal compared to the tree supports, while less dense regions allowed for easier detachment.

Both models were weighed before and after the support structure removal for a weight comparison. The tree supports weigh 108.19 g, while the block supports weigh slightly more at 109.31 g. The masses of the demonstrator parts are 68.79 g and 68.64 g, respectively. These measurements indicate minimal differences in weight between the two support structure types with tree supports being slightly lighter than block supports.

The tree supports facilitated a significantly easier removal of residual powder, with much less powder remaining in the structure compared to block supports, despite undergoing wire erosion under water. The reason for this is the larger free spaces between the tree supports.

4.5 3D scans and process simulations

The demonstrator parts were scanned individually by placing them in the 3D scanning system in a standing position with the help of clamps. Both parts were scanned in two different positions, each time from eight different angles to capture the whole geometry and the scans are combined afterwards in the associated scanning software.

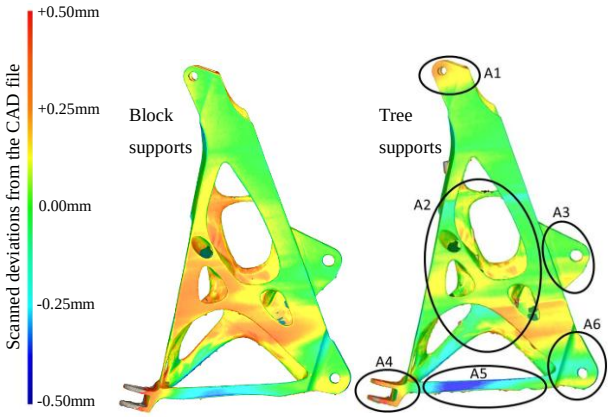

Figure 5: 3D CAD comparison of 3D scanned deviations of the demonstrator part, supported with block supports (l.) and tree supports (r.). The numbered black ovals (A1 – A6) indicate analysed areas.

The scanned data and the original CAD file of the demonstrator are loaded in the scanning software and an internal function is used to align the two models by selecting the same three surfaces (front, bottom and top) of the triangular feature with a hole, seen in the analysed area A3 in Figure 5. A 3D CAD comparison is then generated, showcasing the scanned geometric deviations (+ 0.5 mm to - 0.5 mm) from the original CAD file as a false colour map (Figure 5). Green areas in the colour map represent little to no deviations from the CAD file. Blue and red areas represent major deviations, whereby the blue areas show deviations towards the inside and red areas show deviations towards the outside of the CAD file.

With the help of a preliminary analysis, investigating the results of different referencing locations, a significant influence of the location of alignment on the results of the 3D CAD comparisons could be excluded. Screenshots of this analysis can be found in the supplementary material of this work [23].

To compare the geometrical deviations of the two support structure types (block and tree supports), a total of 30 reference points was created in each model. They were positioned at the same highly displaced or geometrical interesting locations in both models. The local deviations at each of these reference points were saved and summarized in a table, which can be found in the supplementary material of this work, as well as screenshots showing the locations of all reference points [23]. The reference points must not be mistaken with the analysed areas (A1 – A6), which are shown in the right picture of Figure 5 and are used in the following discussion of the scanned results.

In order to facilitate a comparison between the results obtained from 3D scanning and process simulations, an additional 30 reference points were created in both simulated models (Figure 5). These reference points were positioned in the same locations as those used in the previously presented 3D CAD comparison (Figure 6). The evaluation of the deviations at these points was conducted utilising an internal Netfabb function that collects and saves the deviations of all elements contained within drawn rectangles. The mean deviations and their corresponding standard deviations of both parts and from both types of analysis are shown in Table 2.

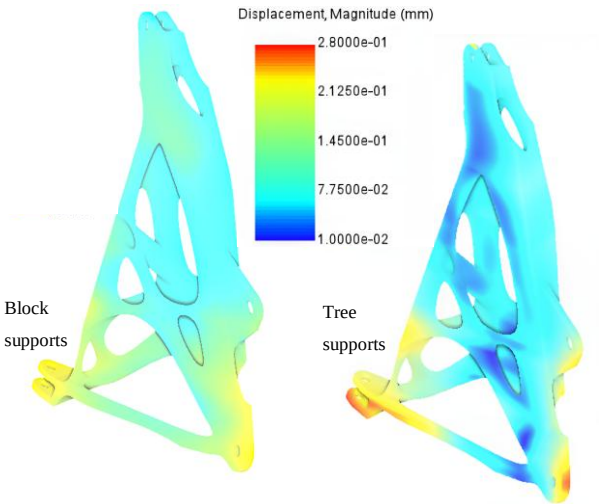

Figure 6: Simulated deviations of the demonstrator part after support removal, supported with block supports (l.) and tree supports (r.)

Figure 6 shows the geometric deviations from original CAD file of the demonstrator after support structure removal, calculated by process simulations. Unlike the 3D CAD comparison results in Figure 5, the legend of these plots does not distinguish between deviations towards the inside and the outside of the original model.

The qualitative comparison of the scanned deviations with the simulated ones showed that the tendencies align in most areas of the demonstrator parts but the general level of deviations is higher in the 3D scanned results for both parts. The mean deviations of the 3D CAD comparison, seen in Table 2 and obtained from the 30 reference points, are 96.24 % and 32.56 % higher than the simulative predicted deviations for block and tree supports, respectively.

The mean deviations of the tree support demonstrator are 34.48 % and 3.01 % smaller than the ones of the block support demonstrator, obtained from the reference points of the 3D scanned and simulated results, respectively (Table 2).

Table 2 Mean deviations and corresponding standard deviations of the demonstrator parts based on 30 reference points from process simulations and 3D scans.

	Simulation		3D scan	
	Block	Tree	Block	Tree
Mean deviation [mm]	0.133	0.129	0.261	0.171
Standard deviation [mm]	0.039	0.062	0.144	0.105

As can be seen in Figure 5 and Figure 6, the demonstrator with block supports shows high deviations in both types of analysis at the feature at the bottom left (A4 in Figure 5) and close to no deviations at the top of the demonstrator (A1) and on the triangular feature on the right side of the part (A3). The latter point is to be expected as the 3D CAD comparison was referenced at that triangular feature. Discrepancies can be recognized in the central area of the part (A2) as well as at the lowest strut (A5) where the scanned results exhibit significantly more deviations than the simulation predicts.

The demonstrator, which was supported by tree supports, exhibits little deviations in the central area (A2) and high deviations at the bottom left feature (A4) in the 3D scanned and the simulated results, whereas the top of the part (A1) and the lowest strut (A5) show a significantly higher level of deviations than the simulation. Contrary to this, the feature at the bottom right (A6) is predicted to show higher deviations than it does in the 3D scan results.

Table 3 Simulated maximum deviations of the demonstrator parts with block and tree supports.

	Block supports	Tree supports
Max. deviation (mag.) after support removal [mm]	0.217	0.279

Contrary to the mean deviations, the simulated maximum deviations (magnitude) of the tree support demonstrator are 28.57 % higher than of the block supports demonstrator (Table 3). This shows that the tree supports lead to reduced mean deviations over the whole part (simulated and 3D scanned) but also to higher local maximum deviations when compared to block supports. The process simulation shows limited capabilities to predict these local maximum deviations, achieving more precise predictions for the tree supports.
Potential reasons for the discrepancies between process simulation results and 3D scans can be attributed to several factors. First, the process parameters used during manufacturing are proprietary and therefore not fully accessible. This likely results in deviations between the actual manufacturing conditions and the process parameters assumed in the simulation, leading to differences in the predicted and observed geometric deviations. Second, alignment challenges during the 3D scanning process may contribute to inaccuracies. Specifically, aligning the scanned model with the CAD reference is particularly difficult in the absence of well-defined geometric features that can serve as precise reference points. Consequently, the reference points used for comparing the simulation and scan results may not perfectly coincide, further exacerbating the observed variations.
The aforementioned limitations underscore the necessity for well-designed reference features to ensure enhanced alignment and measurements with increased accuracy as well as known PBF-LB/M process parameters for improved simulative predictions of the manufacturing process in future studies.

5 Summary and outlook

Novel tree-like support structures were assessed using Ti6Al4V as material in the PBF-LB/M process. The whole manufacturing process of demonstrator parts was simulated and the results were compared to 3D scans of the manufactured samples. An additional parameter study was conducted to evaluate manufacturing limits of thin rods. The following conclusions were drawn:

- Parameter study demonstrated new process limits for PBF-LB/M with Ti6Al4V alloy and extends the design freedom. 50 mm long rods were successfully built with minimum diameters of 0.3 mm and inclination angles to the built platform starting from 20 °, as well as vertical rods of up to 300 mm length with 1.0 mm diameter.
- The examined tree supports performed well on a complex part and 3D scanning of 30 reference points yielded that the manufactured tree supports exhibit 34.48 % less mean deviation than the block supports (0.171 mm compared to 0.261 mm) while being slightly lighter.
- Tree supports enhance work safety significantly compared to commercially widespread block supports as they trapped a lot less powder.
- The mean deviations of the demonstrators, obtained from 30 3D scanned reference points, are 96.24 % and 32.56 % higher than the simulative predicted deviations for block and tree supports, respectively, demonstrating a more accurate prediction for the tree supports. Known process parameters could lead to a significantly increased accuracy of the process simulations and should be analysed in future investigations.
- More precise measurements of the deviations could be achieved by using less organic and less round benchmark parts that allow for a more accurate positioning of the measuring points. Moreover, this approach has the potential to further improve the

precision of the alignment between the scanned models and the CAD file.

- Further research should focus on the trunks of the tree supports that were ending on the component instead of the built plate. The algorithm should be improved to prevent the generation of such trunks.

Acknowledgements

The authors thank the *Insitut für Produktionsmanagement und -technik* (IPMT) of the *Hamburg University of Technology* (TUHH) for making available their 3D scanning system and the *Fraunhofer – Einrichtung für additive Produktionstechnologien* (IAPT) for the design of the block supports and the manufacturing of all parts shown in this work. This research was partly funded by the *Bundesministerium für Bildung und Forschung* (BMBF) as part of the research project "*Bäume als effiziente Stützstrukturen in der additiven Fertigung*" (BEST); grant numbers 02P20E241 and 02P20E240.

Literature

[1] V. C. M. Sobota, G. Van De Kaa, T. Luomaranta, M. Martinsuo, and J. R. Ortt, 'Factors for metal additive manufacturing technology selection', *J. Manuf. Technol. Manag.*, vol. 32, no. 9, pp. 26–47, Dec. 2021, doi: 10.1108/JMTM-12-2019-0448.

[2] I. Gibson, D. Rosen, and B. Stucker, *Additive Manufacturing Technologies: 3D Printing, Rapid Prototyping, and Direct Digital Manufacturing*. New York, NY: Springer New York, 2015. doi: 10.1007/978-1-4939-2113-3.

[3] Wohlers Associates, Ed., *Wohlers report 2019: 3D printing and additive manufacturing state of the industry*. Fort Collins (Colo.): Wohlers Associates, 2019.

[4] M. Salmi, 'Additive Manufacturing Processes in Medical Applications', *Materials*, vol. 14, no. 1, p. 191, Jan. 2021, doi: 10.3390/ma14010191.

[5] C. Sun, Y. Wang, M. D. McMurtrey, N. D. Jerred, F. Liou, and J. Li, 'Additive manufacturing for energy: A review', *Appl. Energy*, vol. 282, p. 116041, Jan. 2021, doi: 10.1016/j.apenergy.2020.116041.

[6] B. Kianian and T. C. Larsson, 'Additive Manufacturing Technology Potential: A Cleaner Manufacturing Alternative', in *Volume 4: 20th Design for Manufacturing and the Life Cycle Conference; 9th International Conference on Micro- and Nanosystems*, Boston, Massachusetts, USA: American Society of Mechanical Engineers, Aug. 2015, p. V004T05A001. doi: 10.1115/DETC2015-46075.

[7] J. A. Slotwinski, 'Additive manufacturing: Overview and NDE challenges', presented at the 40TH ANNUAL REVIEW OF PROGRESS IN QUANTITATIVE NONDESTRUCTIVE EVALUATION: Incorporating the 10th International Conference on Barkhausen Noise and Micromagnetic Testing, Baltimore, Maryland, USA, 2014, pp. 1173–1177. doi: 10.1063/1.4864953.

[8] H. R. Javidrad and F. Javidrad, 'Review of state-of-the-art research on the design and manufacturing of support structures for powder-bed fusion additive manufacturing', *Prog. Addit. Manuf.*, vol. 8, no. 6, pp. 1517–1542, Dec. 2023, doi: 10.1007/s40964-023-00419-6.

[9] J. Jiang, X. Xu, and J. Stringer, 'Support Structures for Additive Manufacturing: A Review', *J. Manuf. Mater. Process.*, vol. 2, no. 4, p. 64, Sep. 2018, doi: 10.3390/jmmp2040064.

[10] M. Zhou, Y. Liu, and C. Wei, 'Topology optimization of easy-removal support structures for additive manufacturing', *Struct. Multidiscip. Optim.*, vol. 61, no. 6, pp. 2423–2435, Jun. 2020, doi: 10.1007/s00158-020-02607-2.

[11] B. Vaissier, J.-P. Pernot, L. Chougrani, and P. Véron, 'Genetic-algorithm based framework for lattice support structure optimization in additive manufacturing', *Comput.-Aided Des.*, vol. 110, pp. 11–23, May 2019, doi: 10.1016/j.cad.2018.12.007.

[12] J. Hünting, J. Waldschmidt, J. Michael, M. Dias Da Silva, C. Emmelmann, and T. Röver, 'Baumstützstrukturen in der additiven Fertigung: Effizienzsteigerung im 3D-Druck und der spanenden Nachbearbeitung komplexer Metallbauteile', *Z. Für Wirtsch. Fabr.*, vol. 118, no. 11, pp. 773–777, Nov. 2023, doi: 10.1515/zwf-2023-1156.

[13] J. Waldschmidt, M. Dias Da Silva, S. Roth, and T. Röver, 'Resource-efficient add-on structures for the mechanical postprocessing of laser powder bed fusion parts using five-axis machining', *J. Laser Appl.*, vol. 36, no. 4, p. 042065, Nov. 2024, doi: 10.2351/7.0001637.

[14] T.-H. Kwok, 'Escaping Tree-Support (ET-Sup): minimizing contact points for tree-like support structures in additive manufacturing', *Rapid Prototyp. J.*, vol. 27, no. 8, pp. 1562–1572, Sep. 2021, doi: 10.1108/RPJ-12-2020-0317.

[15] J. Hünting, J. M. Crego Lozares, M. I. Maiwald, J. Michael, C. Emmelmann, and T. Röver, 'Development of a tree-support software module for PBF-LB/M', in *Proceedings zur Lasers in Manufacturing Konferenz (LiM 2023)*, München, Sep. 2023. [Online]. Available: https://www.wlt.de/2023/proceedings-zur-lasers-manufacturing-konferenz-lim-2023-jetzt-online

[16] K. Bartsch, *Digitalization of design for support structures in laser powder bed fusion of metals*. in Light

Engineering für die Praxis. Springer Nature Switzerland, 2023. doi: 10.1007/978-3-031-22956-5.

[17] R. Feng, X. Li, L. Zhu, A. Thakur, and X. Wei, ‘An Improved Two-Level Support Structure for Extrusion-Based Additive Manufacturing’, *Robot. Comput.-Integr. Manuf.*, vol. 67, p. 101972, Feb. 2021, doi: 10.1016/j.rcim.2020.101972.

[18] Y. Zhang, Z. Wang, Y. Zhang, S. Gomes, and A. Bernard, ‘Bio-inspired generative design for support structure generation and optimization in Additive Manufacturing (AM)’, *CIRP Ann.*, vol. 69, no. 1, pp. 117–120, 2020, doi: 10.1016/j.cirp.2020.04.091.

[19] J. Hünting, J. Michael, M. I. Maiwald, C. Emmelmann, T. Röver, and J. M. Crego Lozares, ‘Supplementary material (Version 2) to publication with title: Development of a tree-support software module for PBF-LB/M’. tore.tuhh.de, Jul. 05, 2023. doi: 10.15480/336.5207.2.

[20] ‘Netfabb Local Simulation - Keyword User Manual Version 2024.0’. Autodesk INC., Feb. 06, 2023.

[21] ‘SLM500 - Production Ready Selective Laser Melting - Optimized for Faster Multi-Laser, Cost-Efficient Builds for High Volume Projects’. SLM Solutions.

[22] ‘Modellreihe VL Optisches 3D-Koordinatenmessgerät Katalog’. Accessed: Aug. 28, 2024. [Online]. Available: https://www.keyence.de/mykeyence/?ptn=001

[23] J. Hünting, J. Michael, C. Emmelmann, and T. Röver, ‘Supplementary material to publication with title: On Resource Efficient and Individualized Tree Support Structures for PBF-LB/M by Process Simulation’. tore.tuhh.de, Dec. 10, 2024. doi: 10.15480/882.13332.

[24] J. D. Arputharaj, S. Nafisi, and R. Ghomashchi, ‘Printability and Geometric Capability of L-Pbf in Manufacturing Thin Circular Cross-Sections’, 2023. doi: 10.2139/ssrn.4598645.

[25] J. Kranz, D. Herzog, and C. Emmelmann, ‘Design guidelines for laser additive manufacturing of lightweight structures in TiAl6V4’, *J. Laser Appl.*, vol. 27, no. S1, p. S14001, Feb. 2015, doi: 10.2351/1.4885235.